

Electronic Supplementary Information

Ultrasensitive photo-driven self-powered aptasensor for microcystin-RR assay based on ZnIn₂S₄/Ti₃C₂ MXene integrated with a matching capacitor for multiple signal amplification

Jun Sun,^{a,} Rongquan Zhu,^a Xiaojiao Du,^{a,b,*} Bing Zhang,^b Min Zheng,^{a,b} Xingyu Ji,^a*

Long Geng^a

^a School of Electrical and Information Engineering, Jiangsu University, Zhenjiang 212013, P. R. China

^b School of Photoelectric Engineering, Changzhou Institute of Technology, Changzhou, Jiangsu, 213032, P. R. China

*Corresponding author.

E-mail address: duxj@czust.edu.cn (X.J. Du)

sun2000jun@ujjs.edu.cn (J. Sun)

Contents.

The pretreatment of the real samples.....	S3
The UV–Vis diffuse-reflectance spectra of ZnIn₂S₄, Ti₃C₂ , and Ti₃C₂/ZnIn₂S₄. (Fig. S1).....	S4
The UV–Vis diffuse-reflectance spectra of apt, Ti₃C₂/ZnIn₂S₄, and apt/Ti₃C₂/ZnIn₂S₄. (Fig. S2).....	S5
The zeta potential diagram of Ti₃C₂/ZnIn₂S₄ (Fig. S3A) before and (Fig. S3B) after adding the MC-RR aptamer.....	S6
The XPS pattern of ZnIn₂S₄ and Ti₃C₂/ZnIn₂S₄, Zn 2p, In 3d, S 2p, Ti 2p, and C 1s. (Fig. S4).....	S7
The OCP curve of ZnIn₂S₄/FTO photoanode and Cu₂O/FTO photocathode with or without photoirradiation. (Fig. S5).....	S8
Effect of pH values of PBS. (Fig. S6).....	S9
The reproducibility of the developed aptasensor toward MC-RR. (Fig. S7)....	S10
Comparison of the proposed self-powered aptasensor for the detection of MC-RR with other methods. (Table S1).....	S11

The pretreatment of the real samples

Live fish samples were purchased from the market in Xinbei District, Changzhou City. The fish was put in 40 °C water, and dead about 5 min. Then the dead fish was placed on the anatomical disc and muscle tissue were taken for experiment use. Fish samples were pretreated before testing.^{1,2} Specifically, fresh fish samples were thoroughly dissected to obtain muscle tissue samples, and the muscle tissue samples were homogenized with a masher to form meat paste samples. Next, 10 g (accurate to 0.01 g) of meat paste samples and anhydrous sodium sulfate (40 g) were placed in a mortar, and ground to a fine powder. The ground fine powder was placed in a stoppered erlenmeyer flask with cyclohexane solution (50 mL), and shook as well as filtered for 20 minutes. To purify the interfering factors such as fat in the real samples,³ concentrated sulfuric acid (5 mL, 80 % by mass) was employed to sulfonation treatment until it was colorless and transparent. And then, to wash and neutralize the real samples solution, the organic phase was added with sodium sulfate solution (2 %, the mass percentage) to stand for separation, and the aqueous layer was removed. After that, the organic phase was dehydrated by anhydrous sodium sulfate (10 g) in a K-D concentrator, and the real samples solution was concentrated to about 0.5 mL, which was sequentially adjusted to 1.0 mL. Moreover, to obtain the required MC-RR spiked samples (1 ~ 100 ng L⁻¹), the corresponding standard concentration of MC-RR (0.1 ~ 100 ng L⁻¹) was added to the extracted real sample solution, and centrifuged at 4000 rpm for 10 minutes. The extracted buffer samples solution was used for MC-RR detection of the proposed aptasensor.

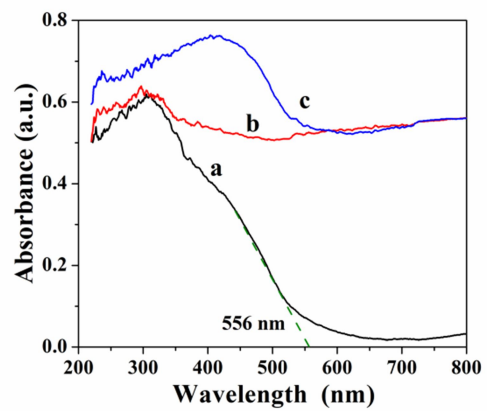


Fig. S1. The UV–Vis diffuse-reflectance spectra of ZnIn_2S_4 (curve a), Ti_3C_2 (curve b), and $\text{Ti}_3\text{C}_2/\text{ZnIn}_2\text{S}_4$ (curve c).

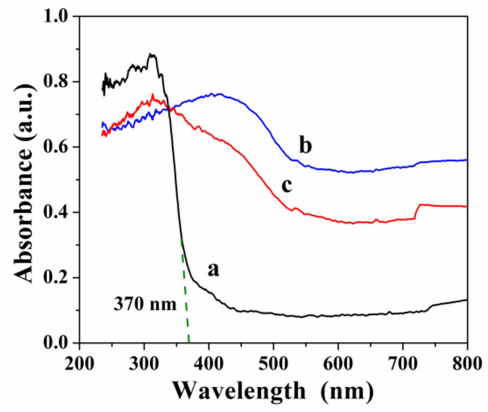


Fig. S2. The UV–Vis diffuse-reflectance spectra of apt (curve a), $\text{Ti}_3\text{C}_2/\text{ZnIn}_2\text{S}_4$ (curve b), and apt/ $\text{Ti}_3\text{C}_2/\text{ZnIn}_2\text{S}_4$ (curve c).

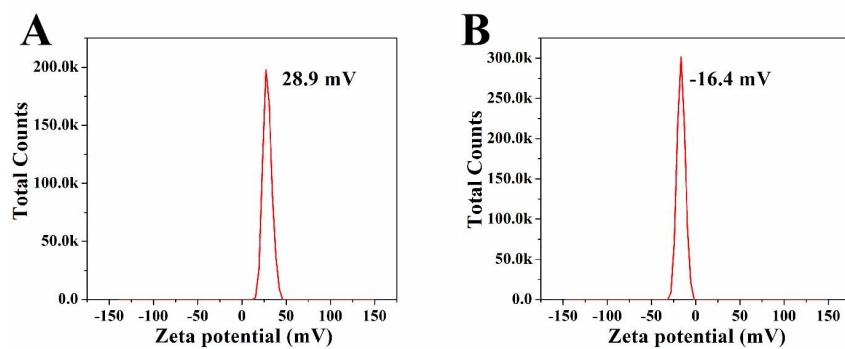


Fig. S3. The zeta potential diagram of $\text{Ti}_3\text{C}_2/\text{ZnIn}_2\text{S}_4$ (A) before and (B) after adding the MC-RR aptamer.

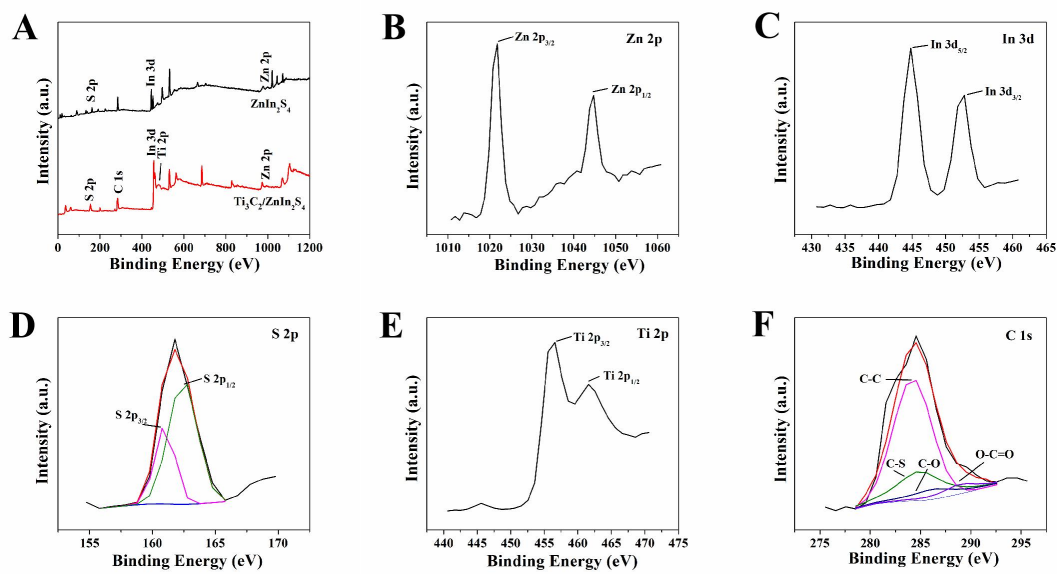


Fig. S4. (A) The XPS pattern of ZnIn₂S₄ and Ti₃C₂/ZnIn₂S₄, (B) Zn 2p, (C) In 3d, (D) S 2p, (E) Ti 2p, and (F) C 1s.

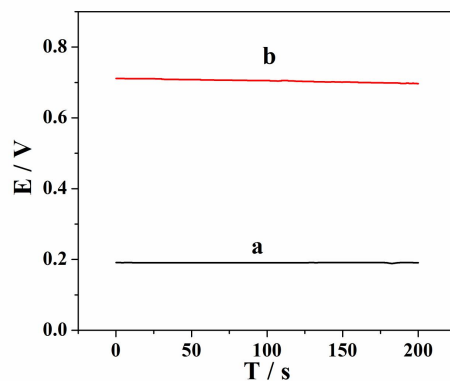


Fig. S5. The OCP curve of ZnIn₂S₄/FTO photoanode and Cu₂O/FTO photocathode with (curve a) or without (curve b) photoirradiation in 0.1M PBS (6.0).

The OCP value of the proposed aptasensor is ≈ 0.71 V under the photoirradiation condition, which is much higher than the OCP value of 0.18 V in the dark environment, suggesting that excitation light source plays an crucial role in the whole sensing platform. The explanation of the result is that the excitation light source drives the separation between electron-hole on the surface of the ZnIn₂S₄ photoanode, thereby accelerating the migration rate of photoelectrons from the photoanode to the photocathode and improving the photoelectric conversion efficiency.

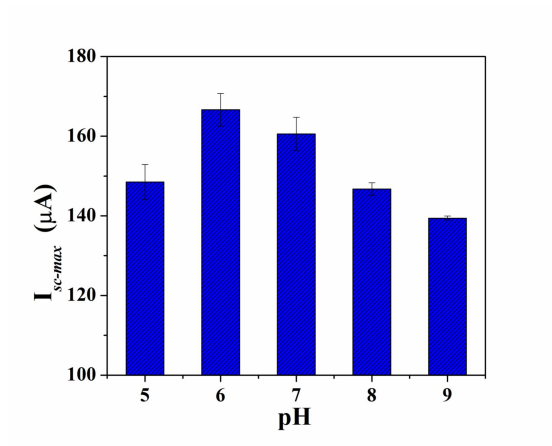


Fig. S6. Effect of pH values of PBS.

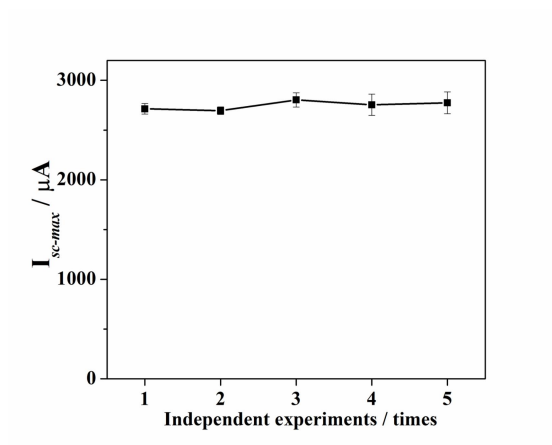


Fig. S7. The reproducibility of the developed aptasensor toward MC-RR at 1 pM concentration.

Table S1 Comparison of the proposed self-powered aptasensor for the detection of MC-RR with other methods.

Methods	Linear range (mol/L)	LOD (mol/L)	Reference
Multi-immunogen	$1.7 \times 10^{-7} \sim 2.7 \times 10^{-6}$	8.0×10^{-8}	[4]
CL ^a aptasensor	$1.0 \times 10^{-10} \sim 7.0 \times 10^{-8}$	3.3×10^{-11}	[5]
Fluorometric	$2.0 \times 10^{-7} \sim 2.5 \times 10^{-6}$	8.0×10^{-8}	[2]
FMIP ^b Mn doped ZnS QDs	$2.5 \times 10^{-9} \sim 1.8 \times 10^{-8}$	6.0×10^{-13}	[6]
Au@label@Ag@Au NPs	$1.0 \times 10^{-11} \sim 1.0 \times 10^{-9}$	1.3×10^{-12}	[7]
Self-powered aptasensor	$1.0 \times 10^{-13} \sim 1.0 \times 10^{-10}$	3.3×10^{-14}	This work

a—Chemiluminescence

b—Fragment-dummy-template molecularly imprinted polymers

References

1. X.J. Du, W.H. Du, J. Sun and D. Jiang, *Food Chem.*, 2022, **385**, 132731.
2. S.J. Wu, Q. Li, N. Duan, H.L. Ma and Z.P. Wang, *Microchim. Acta*, 2016, **183**, 2555–2562.
3. C.Z. Zhang, P.C. Chen, L.Y. Zhou and J.Y. Peng, *Food Chem.*, 2022, **366**, 130490.
4. J.C. Liu, Y.H. Yang, Q. Zhu, Z.H. Wang, G.J. Hu, H.C. Shi and X.H. Zhou, *Environ. Sci. Technol.*, 2021, **55**, 12984–12993.
5. B.R. Liu, X.H. Li, S.M. Liu and X. Hun, *Microchem. J.*, 2019, **145**, 648–654.
6. Y.Y. Li, J.Q. You, Y. He, Y.L. Ge, G.W. Song and J.G. Zhou, *ChemistrySelect.*, 2020, **5**, 12028–12033.
7. X.J. Lou, X.J. Zhao, G.Q. Wallace, M.H. Brunet, K.J. Wilkinson, P. Wu, C.X. Cai, C.G. Bazuin and J.F. Masson, *ACS Appl. Mater. Interfaces.*, 2021, **13**, 6545–6556.